Layering transitions in the Abraham model

1994 J. Phys. A: Math. Gen. 27 2939

(http://iopscience.iop.org/0305-4470/27/9/011)

J. Phys. A: Math. Gen. 27 (1994) 2939–2952. Printed in the UK

Layering transitions in the Abraham model

C L O'Donnell and J M Yeomans

Theoretical Physics, University of Oxford, 1 Keble Road, Oxford OX1 3NP, UK

Received 18 November 1993

Abstract. We show by means of a low-temperature series expansion that a large, possibly infinite number of interface layering transitions are observed for the Abraham model in dimensions $d \geqslant 3$.

1. Introduction

In this paper we consider an interface unbinding from a surface at low temperatures in the $(d \geqslant 3)$-dimensional Abraham model [1]. We are working below the roughening temperature and the effect of the lattice is that unbinding, or wetting, can take place through a series of first-order steps or layering transitions [2, 3]. Our aim is to use a low-temperature series approach, first introduced for interface problems by Duxbury and Yeomans [4], and based on work by Fisher and Selke [5], to understand the structure of the layering transitions in the Abraham model and their dependence on the co-ordination number of the lattice.

A wetting transition that takes place as a bulk field tends to zero is called complete wetting. For the three-dimensional Ising model with short-range interactions, Duxbury and Yeomans [4] showed that complete wetting takes place through an infinite series of layering transitions.

Another possibility is that the unbinding transition should be driven by a varying surface field. The paradigm of this case for the Ising system is the Abraham model where the interface is pinned by a surface field. Here the situation has remained unclear. In their treatment of the model, Duxbury and Yeomans [4] were able to establish the existence of one layering transition but did not carry the low-temperature series to high enough order to predict whether or not more transitions were stable. Armitstead and Yeomans [6] found that for a solid-on-solid version of the model, where overhangs of the interface and bulk fluctuations were neglected, an infinite series of layering transitions could be established. A Monte Carlo investigation by Binder and Landau [7] provided evidence for two layering transitions. They speculated on the possibility of a larger number lying beyond the resolution of the numerical approach.

Therefore the aim of this work is to reconsider the Abraham model in $d \geqslant 3$ at low temperatures to understand more fully how the wetting transition comes about. We show that the difficulty in using a low-temperature series approach to treat this problem arises because a given phase is stabilized only at a relatively high order of the expansion compared to the distance of the interface from the surface. Therefore many diagrams contribute to the free-energy difference between phases with different interface positions making a general-order calculation prohibitively difficult.

We are able to establish that there are at least four layering transitions in the Abraham model on a simple cubic lattice. Using a simplified version of the model an argument for

0305-4470/94/092939+14$19.50

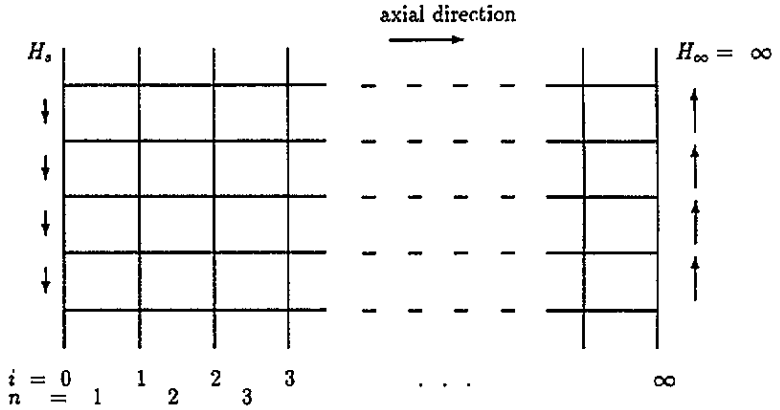

Figure 1. Schematic representation of the Abraham model. i labels the planes perpendicular to the axial direction and n the position of the interface.

the existence of a large, probably infinite sequence beyond this is proposed. We consider the dependence of our results on the co-ordination number of the lattice and demonstrate that the qualitative nature of the layering transitions is unaltered. Hence, to the order we can take the calculations, mean-field theory gives a qualitatively correct representation of the low-temperature phase diagram.

2. The Abraham model

Consider a d-dimensional lattice with periodic boundary conditions in $(d-1)$ directions. An interface is introduced perpendicular to the special or axial direction by imposing an infinite surface field at one end and a finite field of opposite sign at the other as shown in figure 1. Ising spins $S_{i,j} = \pm 1$ interact through the Abraham model Hamiltonian

$$H = -J \sum_{i,j} S_{i,j} S_{i+1,j} - J_0 \sum_{i,j,j'} S_{i,j} S_{i,j'} + H_s \sum_{j} S_{0,j} \tag{1}$$

where the pair interactions are ferromagnetic and extend over nearest-neighbour sites. The subscript i labels the layers along the axial direction with $i = 0$ being the surface layer. J is the interaction between layers and J_0 the interaction within each layer. We use n to label the position of the interface with $n = 0$ describing the situation with no interface. Let $q_\perp$ be the co-ordination number within the layers. For a hypercubic lattice $q_\perp = 2(d-1)$. The co-ordination number along the axial direction will be taken equal to 2.

The layering transitions in the Abraham model are driven by the surface field, H_s. For $H_s < J$ the ground state is $n = 0$ (no interface). For $H_s = J$ all positions of the interface are degenerate at zero temperature. For $H_s > J$ all phases $n \geqslant 1$ are degenerate. At finite temperature, entropic contributions to the free energy will break this degeneracy possibly leading to a sequence of first-order layering transitions. This is shown schematically in figure 2. In the next section we show how these contributions can be calculated using a low-temperature series expansion.

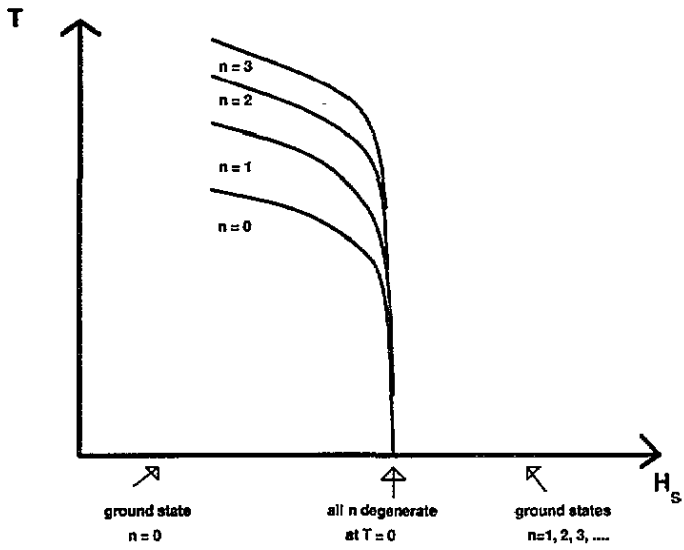

Figure 2. Schematic low-temperature phase diagram of the Abraham model in dimensions $d \geqslant 3$.

3. The low-temperature series expansion

To establish the existence of a sequence of layering transitions, the phase diagram for the Abraham model must be studied at non-zero temperatures. This involves the consideration of spin flips about all degenerate ground states. The low-temperature expansion follows as usual from a decomposition of the the partition function [8]

$$Z_n(N) = \exp\left(\frac{-NE_n^0}{k_B T}\right)\left[1 + \sum_{m=1} \Delta Z_n^m(N)\right] \tag{2}$$

where n labels the position of the interface at $T = 0$, E_n^0 is the ground-state energy per spin for the interface in position n, N is the total number of spins in the lattice, k_B is Boltzmann's constant and $\Delta Z_n^m(N)$ is the total contribution from states with m overturned spins. The reduced free-energy per spin is given by

$$f_n = \frac{-F_n(N)}{Nk_B T} = \frac{-E^0}{k_B T} + \sum_{m=1}' \frac{\Delta Z_n^m(N)}{N} \tag{3}$$

where the prime on the summation indicates that only terms which are linear in N are included, a consequence of the linked-cluster theorem [8].

Even for rather small values of m, listing and counting all the different spin configurations with their associated Boltzmann weights is a substantial task. The simplification pertinent to the present problem is to *compare* the free energies of two different interfacial positions. The majority of the contributions to the individual free energies will be the same for both values of n and we need only concentrate on the much smaller number of terms which contribute in leading order to the free-energy difference.

The Boltzmann factors which appear in the expansion are:

$x = \exp(-2\beta J)$: the contribution for introducing a wrong bond perpendicular to the interface

$\omega = \exp(-2\beta J_0)$: for introducing a wrong bond parallel to the interface

$h_s = \exp(-2\beta H_s)$: for flipping a surface spin away from the field direction.

The aim is to find the interface position n which, for a given H_s and T, maximizes the reduced free energy. The summation in (3) may be expressed as a power series in the parameter ω. We assume that the intra-planar interactions are strong enough so that ω is sufficiently small that the form of the phase diagram may be deduced from the leading-order terms of the expansion, with higher-order corrections yielding only a small shift of the phase boundaries.

4. Phase boundaries

To investigate the low-order layering transitions of the Abraham model we expand h_s in terms of $\omega^{q_\perp}$

$$h_s = x(1 + \alpha_1\omega^{q_\perp} + \alpha_2\omega^{2q_\perp-2} + \alpha_3\omega^{2q_\perp} + \alpha_4\omega^{3q_\perp-4} + \alpha_5\omega^{3q_\perp-2} + \alpha_6\omega^{3q_\perp} + \alpha_7\omega^{4q_\perp-6} + \cdots) \tag{4}$$

and consider in turn $\alpha_1, \alpha_2, \ldots$. In general, on a lattice with no loops, the expansion of h_s will contain terms $O(\omega^{nq_\perp-2m})$ where $n = 1, 2, 3, \ldots$ and $m = n-1, n-2, \ldots, 1, 0$. It follows immediately from (4) that

$$-2\beta H_s = -2\beta J + \alpha_1\omega^{q_\perp} + \alpha_2\omega^{2q_\perp-2} + \left(\alpha_3 - \tfrac{1}{2}\alpha_1^2\right)\omega^{2q_\perp} + \alpha_4\omega^{3q_\perp-4} + (\alpha_5 - \alpha_1\alpha_2)\omega^{3q_\perp-2} + \left(\alpha_6 - \alpha_1\alpha_3 + \tfrac{1}{3}\alpha_1^3\right)\omega^{3q_\perp} + \alpha_7\omega^{4q_\perp-6} + \cdots . \tag{5}$$

Where it is necessary to distinguish a particular phase boundary, between interface phases $n+1$ and n, say, we shall write $(\beta H_s)_{n+1:n}$, $(\alpha_1)_{n+1:n}$ and so on.

4.1. Calculation of α_1

The first step is to calculate $(\alpha_1)_{n+1:n}$ and show that it is independent of n. Consider which diagrams contribute to the reduced free-energy difference $f_{n+1} - f_n$. Only certain diagrams which span the distance between the interface and the surface do not drop out when the free-energy difference is taken. Physically this is reasonable: only those excitations of the interface which lead to its touching the surface can carry information about its position relative to the surface. Of these, those which contribute at lowest order are certain axial chains of length n, shown in figure 3. All possible diagrams corresponding to disconnections of the axial chains must also be included (see figure 4). It follows from the linked-cluster theorem that each disconnection is associated with a factor of -1 [5]. The axial chains of length n give a contribution to $f_{n+1} - f_n$ of

$$(1 - x^2 + h_s x - h_s x^{-1})(1 - x^2)^{n-1}\omega^{nq_\perp} \qquad n \geqslant 1 . \tag{6}$$

Using (4) to substitute for h_s it is immediately apparent that the leading term in (6) is $O(\omega^{(n+1)q_\perp})$ not $O(\omega^{nq_\perp})$. Other diagrams will be relevant at this order. It is easy to check that all other diagrams of length n along the axial direction give a contribution of at least $O(\omega^{(n+2)q_\perp})$. Of the diagrams that span $n+1$ sites, only certain axial chains of length $n+1$, together with their disconnections, need be considered $O(\omega^{(n+1)q_\perp})$. The relevant diagrams are shown in figure 5. Putting the resulting term together with (6) and using (4) gives

$$f_{n+1} - f_n = \{(1 - x^2)^{n+1} - \alpha_1(1 - x^2)^n\}\omega^{(n+1)q_\perp} + O(\omega^{(n+2)q_\perp}) \qquad n \geqslant 1 . \tag{7}$$

On the boundary between n and $n+1$ the free-energy difference must be zero. Hence

$$\alpha_1 = (1 - x^2) \tag{8}$$

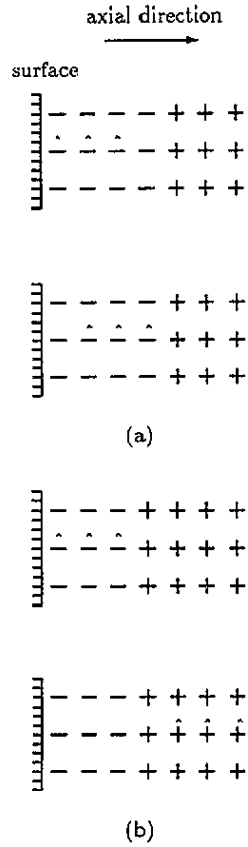

Figure 3. Diagrams which contribute to the reduced free-energy difference $f_{n+1} - f_n$ at $O(\omega^{nq_\perp})$ (shown here for $n = 3$). Spins $S_i = -1, +1$ are denoted by $-, +$ respectively. A caret denotes a spin flip. (*a*) Contributions from f_{n+1}. (*b*) Contributions from f_n which carry a factor (-1) when the difference is taken.

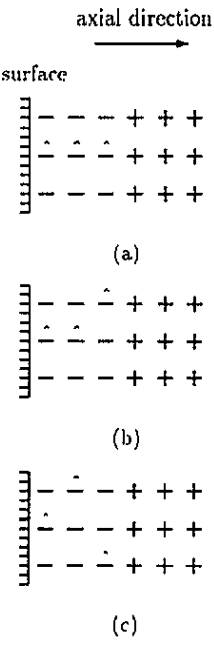

Figure 4. Example of (*a*) a connected diagram $O(\omega^{3q_\perp})$ and, (*b*) and (*c*), corresponding axially disconnected diagrams which carry factors of (-1) and $(-1)^2$ respectively.

for all $n \geqslant 1$.

The free-energy difference $f_1 - f_0$ can be calculated in a similar way. Considering only single spin flips

$$f_1 - f_0 = 2\beta(H_s - J) + (1 - x^2 + h_s x^{-1} - h_s^{-1} x)\omega^{q_\perp} + O(\omega^{2q_\perp - 2}) \qquad (9)$$

and it follows immediately from the leading-order terms in (4) and (5) that the expression (8) for α_1 also holds for $n = 0$. Hence to this order there is a *shift* but no *splitting* of the phase boundary between the phases $n = 0$ and $n \geqslant 1$.

Proceeding to higher orders the calculation rapidly becomes more complex and it will be helpful to summarize the contributing diagrams in tabular form. The relevant diagrams $O(\omega^{(n+1)q_\perp})$, which are needed to calculate α_1, are shown in table 1 for $n = 1, 2, 3, 4$. A caret denotes a flipped spin. The table gives the topology of the relevant diagrams. However, they must be positioned correctly relative to the interface for their contribution not to drop out when the free-energy difference is taken. All axial disconnections must be taken into account. The quantity α_1 at the beginning of a row indicates that the corresponding diagrams

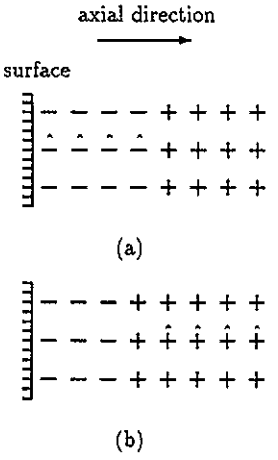

Figure 5. Diagrams which contribute to the reduced free-energy difference $f_{n+1} - f_n$ at $O(\omega^{(n+1)q_\perp})$ (shown here for $n = 3$). (*a*) Contributions from f_{n+1}. (*b*) Contributions from f_n which carry a factor (-1) when the difference is taken.

Table 1. Diagrams which contribute to the free-energy differences $f_{n+1} - f_n$, $n = 0, 1, 2, 3$ at $O(\omega^{(n+1)q_\perp})$. A caret denotes a flipped spin. The diagrams must be placed on the lattice such that they form chains along the axial direction and must lie in the correct position relative to the interface for their contribution not to cancel out when the free-energy difference is taken. All axial disconnections must be taken into account. Rows labelled α_n contribute to the required order when the term in the expansion of h_s proportional to α_n is substituted into the contribution from the diagram.

	$f_1 - f_0$	$f_2 - f_1$	$f_3 - f_2$	$f_4 - f_3$
-	^	‾	‾‾	‾‾‾
α_1	-	^	‾	‾‾

Table 2. Contributing diagrams at $O(\omega^{(n+2)q_\perp - 2})$.

	$f_1 - f_0$	$f_2 - f_1$	$f_3 - f_2$	$f_4 - f_3$
-	^	^^	^^^	^^^^
α_1	-	^	^^	^^^
α_2	-	^	^^	^^^

give a contribution to the free energy difference $O(\omega^{(n+1)q_\perp})$ and proportional to α_1 when h_s is expanded $O(\omega^{q_\perp})$.

4.2. *Calculation of* α_2

To calculate α_2, terms $O(w^{(n+2)q_\perp - 2})$ in the reduced free-energy differences are needed. The relevant diagrams, for low n, are listed in table 2. As before, the diagrams must be positioned correctly relative to the interface for their contribution not to drop out when the free-energy difference is taken. Axial, but not in-plane disconnections must be included: the latter contribute to higher order in ω. The rows labelled α_1 and α_2 in table 2 give a contribution to the required order when the terms in h_s of $O(\omega^{q_\perp})$ and $O(\omega^{2q_\perp - 2})$ respectively from (4) are substituted into the free-energy difference.

Summing the contributions from the graphs listed in table 2 and using equations (4) and

(8) gives the term $O(\omega^{(n+2)q_\perp-2})$ in $f_{n+1}-f_n$

$$\begin{aligned} &\left\{\frac{q_\perp}{2}(1-x^4)-2\alpha_2\right\} && n=0\\ &\{q_\perp x^2(1-x^2)^n-\alpha_2(1-x^2)^{n-1}\} && n\geqslant 1 \end{aligned}$$

from which it follows immediately that

$$\begin{aligned} (\alpha_2)_{1:0} &= \frac{q_\perp}{2}(1-x^4)\\ (\alpha_2)_{n+1:n} &= q_\perp x^2(1-x^2) \qquad n\geqslant 1\,. \end{aligned} \tag{10}$$

Equation (10) shows that there is a splitting of the boundaries. Hence at this order $n=1$ has been shown to be a stable phase. All phases with $n\geqslant 1$ remain degenerate on the $1:\infty$ boundary.

4.3. Higher order terms

The calculation proceeds iteratively with terms in the free-energy differences $O(\omega^{(n+m)q_\perp-p})$ enabling the calculation of the coefficient $O(\omega^{mq_\perp-p})$ in the expansion (4) of h_s. The diagrams which contribute at each order are listed in tables 3–7. The number and complexity of the diagrams increases quickly as the expansion proceeds. Calculating the contribution to the low-temperature series from each diagram is laborious but not difficult. In each case it comprises the count together with the Boltzmann factor for the diagram placed at the appropriate position on the lattice relative to the interface. In every case all axial disconnections must be included. In-plane disconnections contribute explicitly to the order of the graph and are marked in the tables by a horizontal bar. A list of the contributions of each graph is available [9].

Table 3. Contributing diagrams at $O(\omega^{(n+2)q_\perp})$; a bar represents an in-plane disconnection.

	f_1-f_0	f_2-f_1	f_3-f_2	f_4-f_3
α_1				
α_1				
α_3				

Table 4. Contributing diagrams at $O(\omega^{(n+3)q_\perp-4})$.

	f_1-f_0	f_2-f_1	f_3-f_2	f_4-f_3
α_1				
α_1				
α_2				
α_4				

Table 5. Contributing diagrams at $O(\omega^{(n+3)q_\perp-2})$.

	$f_1 - f_0$	$f_2 - f_1$	$f_3 - f_2$	$f_4 - f_3$
-				
-				
-	-			
α_1				
α_1	-			
α_1	-	-		
α_2				
α_2	-			
$\alpha_3, \alpha_1{}^2$	-			
α_5	-			

Table 6. Contributing diagrams at $O(\omega^{(n+3)q_\perp})$.

	$f_1 - f_0$	$f_2 - f_1$	$f_3 - f_2$	$f_4 - f_3$
-				
-				
-				
-	-			
α_1				
α_1				
α_1	-			
α_1	-	-		
α_3				
$\alpha_3, \alpha_1{}^2$	-			
α_6	-			

It has been possible to obtain results $O(\omega^{(n+4)q_\perp-6})$ and hence to calculate $(\alpha_1)_{n+1:n} \ldots (\alpha_7)_{n+1:n}$ for $n = 0, 1, 2, 3$:

$$(\alpha_1)_{1:0} = (\alpha_1)_{2:1} = (\alpha_1)_{3:2} = (\alpha_1)_{4:3} = 1 - x^2 \tag{11}$$

$$\begin{aligned}(\alpha_2)_{1:0} &= \tfrac{1}{2}q_\perp(1 - x^4)\\ (\alpha_2)_{2:1} &= (\alpha_2)_{3:2} = (\alpha_2)_{4:3} = q_\perp x^2(1 - x^2)\end{aligned} \tag{12}$$

$$\begin{aligned}(\alpha_3)_{1:0} &= (1 - x^2)[(1 - 2x^2) - \tfrac{1}{2}q_\perp(1 + x^2)]\\ (\alpha_3)_{2:1} &= (\alpha_3)_{3:2} = (\alpha_3)_{4:3} = (1 - x^2)[(1 - 2x^2) - q_\perp x^2]\end{aligned} \tag{13}$$

$$\begin{aligned}(\alpha_4)_{1:0} &= \tfrac{1}{2}q_\perp(q_\perp - 1)(1 - x^6)\\ (\alpha_4)_{2:1} &= \tfrac{1}{2}q_\perp(1 - x^2)[(1 - 4x^4) + 3q_\perp x^4]\\ (\alpha_4)_{3:2} &= (\alpha_4)_{4:3} = \tfrac{1}{2}q_\perp x^2(1 - x^2)[2 - 5x^2 + 3q_\perp x^2]\end{aligned} \tag{14}$$

Table 7. Contributing Diagrams at $O(\omega^{(n+4)q_\perp-6})$.

	$f_1 - f_0$	$f_2 - f_1$	$f_3 - f_2$	$f_4 - f_3$
				
				
α_1				
α_1				
α_1				
α_2				
α_2				
α_3				
α_7				

$$
\begin{aligned}
(\alpha_5)_{1:0} &= -{q_\perp}^2(1-x^6) + \tfrac{1}{2}q_\perp(1-x^2)^2(3+5x^2) \\
(\alpha_5)_{2:1} &= -\tfrac{1}{2}q_\perp(1-x^2)[(1-x^2)(1-5x^2) + 6q_\perp x^4] \\
(\alpha_5)_{3:2} &= (\alpha_5)_{4:3} = q_\perp x^2(1-x^2)[2(1-x^2) - 3q_\perp x^2]
\end{aligned}
\tag{15}
$$

$$
\begin{aligned}
(\alpha_6)_{1:0} &= (1-x^2)(4-8x^2+5x^4) + \tfrac{1}{2}{q_\perp}^2(1-x^6) - \tfrac{1}{2}q_\perp(1-x^2)(2+x^2-6x^4) \\
(\alpha_6)_{2:1} &= (\alpha_6)_{3:2} = (\alpha_6)_{4:3} = (1-x^2)[(1-5x^2+5x^4) + \tfrac{3}{2}{q_\perp}^2x^4 - \tfrac{3}{2}q_\perp x^2(2-3x^2)]
\end{aligned}
\tag{16}
$$

$$
\begin{aligned}
(\alpha_7)_{1:0} &= \tfrac{1}{2}q_\perp(1-q_\perp)^2(1-x^8) \\
(\alpha_7)_{2:1} &= -\tfrac{1}{2}q_\perp(1-x^2)[2(1+x^2-4x^6) - 4{q_\perp}^2x^6 - q_\perp(1+x^2+x^4-11x^6)] \\
(\alpha_7)_{3:2} &= \tfrac{1}{2}q_\perp(1-x^2)[(1-x^2-11x^4+15x^6) + 2q_\perp x^4(3-7x^2) + 4{q_\perp}^2x^6] \\
(\alpha_7)_{4:3} &= q_\perp x^2(1-x^2)[(1-7x^2+8x^4) + q_\perp x^2(3-7x^2) + 2{q_\perp}^2x^4] .
\end{aligned}
\tag{17}
$$

It is apparent from these results that the first difference in the 0:1 and 1:2 boundaries is in the coefficient α_2. Hence the width of the interface phase $n = 1$ is $O(\omega^{2q_\perp-2})$. Similarly, the 1 : 2 and the 2 : 3 boundaries are distinguished by α_4 and the $n = 2$ phase has width $O(\omega^{3q_\perp-4})$. The 2 : 3 and 3 : 4 boundaries are distinguished by α_7 and the $n = 3$ phase has width $O(\omega^{4q_\perp-6})$. This pattern suggests that there is indeed a sequence of layering transitions with the interface phase n having a width $O(\omega^{(n+1)q_\perp-2n})$. Further evidence for this assertion is given in section 6 where a simplified version of the Abraham model is considered for which it is possible to take the expansion to higher orders.

5. The simple cubic lattice

The results for the phase boundaries presented in section 4 refer to a lattice without closed loops. On any physically realistic lattice, diagrams which include such loops will be important as the series is taken to higher orders. As an example of the role of loop diagrams we consider the case of the simple cubic lattice. We find, for this case at least, that these diagrams shift the positions of the phase boundaries but do not affect the pattern of the splitting.

For the simple cubic lattice we shall need to include in (4) the additional terms

$$x(\alpha_8\omega^{4q_\perp-8} + \alpha_9\omega^{5q_\perp-10} + \alpha_{10}\omega^{6q_\perp-14}) . \tag{18}$$

The looped diagrams which occur at lowest order are rings of four spins lying within the same layer with attached chains running along the axial direction. They contribute $O(\omega^{(n+4)q_\perp-8})$. Using a tilde to represent such a ring, the relevant diagrams are listed in table 8. We shall also need diagrams $O(\omega^{(n+5)q_\perp-10})$ and $O(\omega^{(n+6)q_\perp-14})$ which are listed in tables 9 and 10. The notation $\tilde{\tilde{}}$ is used to denote six spins within a layer arranged in two rings of four spins which share a side. Summing the contribution from these diagrams and using (18) gives

$$\begin{aligned}
&(\alpha_8)_{1:0} = (1-x^8)\\
&(\alpha_8)_{n+1:n} = 4(1-x^2)x^6 \qquad n = 1,2,3\\
&(\alpha_9)_{1:0} = 8(1-x^{10})\\
&(\alpha_9)_{2:1} = 4(1-x^2)(1+x^4+8x^8)\\
&(\alpha_9)_{n+1:n} = 8(1-x^2)x^6(3+2x^2) \qquad n = 2,3\\
&(\alpha_{10})_{1:0} = 2(1-x^{12})\\
&(\alpha_{10})_{n+1:n} = 12x^{10}(1-x^2) \qquad n = 1,2,3\,.
\end{aligned} \tag{19}$$

Table 8. Additional contributions $O(\omega^{(n+4)q_\perp-8})$ which appear for the simple cubic lattice. $\tilde{}$ denotes a ring of four spins perpendicular to the axial direction.

	f_1-f_0	f_2-f_1	f_3-f_2	f_4-f_3
-	-	-	-	-
α_1	-	-	-	-
α_8	-	^	^^	^^^

Table 9. Additional contributions $O(\omega^{(n+5)q_\perp-10})$ which appear for the simple cubic lattice.

	f_1-f_0	f_2-f_1	f_3-f_2	f_4-f_3
-	~	~	~	~
-	-	-^	-^	-^
α_1	-	~	~	~
α_1	-	-	-^	-^
α_2	-	-	-	-
α_8	-	^	^	^^
α_9	-	^	^^	^^^

Putting $q_\perp = 4$ the diagrams listed in tables 1 and 2 still provide the only contributions at $O(\omega^{4n+4})$ and $O(\omega^{4n+6})$ respectively, but the diagrams listed in tables 3, 4 and 8 all contribute at $O(\omega^{4n+8})$ and those in tables 5, 7, 9 and 10 at $O(\omega^{4n+10})$. Therefore, for the simple cubic lattice, if we define

$$h_s = x(1+\gamma_1\omega^4+\gamma_2\omega^6+\gamma_3\omega^8+\gamma_4\omega^{10}+\cdots) \tag{20}$$

the γs are related to the αs by

$$\gamma_1 = \alpha_1 \qquad \gamma_2 = \alpha_2 \qquad \gamma_3 = \alpha_3+\alpha_4+\alpha_8 \qquad \gamma_4 = \alpha_5+\alpha_7+\alpha_9+\alpha_{10}\,. \tag{21}$$

Table 10. Additional contributions $O(\omega^{(n+6)q_\perp-14})$ which appear for the simple cubic lattice. ⌶ denotes a ring of six spins lying in a plane perpendicular to the axial direction which form two rings of four spins sharing an edge.

	f_1-f_0	f_2-f_1	f_3-f_2	f_4-f_3
.	⌶	⌶	⌶	⌶
α_1	-	⌶	⌶	⌶
α_{10}	-	^	^^	^^^

It follows immediately from (11)–(21) that

$$
\begin{aligned}
(\gamma_1)_{n+1:n} &= 1-x^2 \qquad n=0,1,2,3\\
(\gamma_2)_{1:0} &= 2(1-x^4)\\
(\gamma_2)_{n+1:n} &= 4x^2(1-x^2) \qquad n=1,2,3\\
(\gamma_3)_{1:0} &= (1-x^2)(6+3x^2+7x^4+x^6)\\
(\gamma_3)_{2:1} &= (1-x^2)(3-6x^2+16x^4+4x^6)\\
(\gamma_3)_{n+1:n} &= (1-x^2)(1-2x^2+14x^4+4x^6) \qquad n=2,3\\
(\gamma_4)_{1:0} &= 2(1-x^2)(9+8x^2+x^4+14x^6+5x^8+x^{10})\\
(\gamma_4)_{2:1} &= 2(1-x^2)(3+8x^2-23x^4+28x^6+16x^8+6x^{10})\\
(\gamma_4)_{3:2} &= 2(1-x^2)(1+3x^2-15x^4+35x^6+8x^8+6x^{10})\\
(\gamma_4)_{4:3} &= 4x^2(1-x^2)(3-9x^2+18x^4+4x^6+3x^8)\,.
\end{aligned}
\tag{22}
$$

Regrouping the terms in this way shows that the results are quantitatively the same for the simple cubic lattice and for the lattice without loops.

6. A simplified model

The results of the previous sections suggest that there is an infinite sequence of layering transitions in the Abraham model for general $q_\perp$. However, because of the complexity of the calculation, it has only been possible to show this explicitly for a small number of phases. To test our assertion further, we define a simplified version of the Abraham model where it is possible to demonstrate the existence of a larger number of layering transitions.

We do this by restricting the number of excitations in the model whilst still retaining those thought to be important for layering. All disconnected diagrams and all diagrams with more than two flipped spins in any given layer are ignored. It is then possible to calculate the contribution of the remaining diagrams rather simply by using a transfer-matrix approach first introduced by Yeomans and Fisher [10]. For this model we are able to find explicitly for $n \leqslant 5$ that interface phases of width $O(\omega^{(2n+1)q_\perp-2n})$ are stable and that the pattern of splitting remains the same. In each case the αs defined in (4) agree to leading order with those obtained for the full model, at least to where the splitting has occurred, suggesting very strongly that the correct physics is not lost in the simplification.

The transfer matrices we shall use build up the chain of flipped spins a layer at a time. Each matrix adds the flipped spins within a layer together with the corresponding Boltzmann weights. Multiplying the matrices together builds up the Boltzmann weights for all possible diagrams, given the initial and final states. Consider the matrix $\mathbf{M}_1$, which adds a layer of

up (down) spins to a previous layer of up (down) spins. The rows of the matrix are labelled by the number of spin flips in the first layer, the columns by the number in the second layer. We consider the chain to be built up from left to right:

$$\mathbf{M}_1 = \begin{array}{c} \\ \hat{\uparrow} \\ \hat{\hat{\uparrow}} \end{array} \begin{array}{c} \begin{array}{cc} 1^{\text{st}}\text{ layer} & \qquad \end{array} \\ \begin{pmatrix} \omega^{q_\perp} & q_\perp x \omega^{q_\perp} \\ 2x\omega^{2q_\perp - 2} & \{1 + 2(q_\perp - 1)x^2\}\omega^{2q_\perp - 2} \end{pmatrix} \end{array} \begin{array}{c} \\ \begin{array}{cc} 2^{\text{nd}}\text{ layer} & \qquad \end{array} \\ \begin{array}{cc} \hat{\uparrow} & \hat{\hat{\uparrow}} \end{array} \end{array}.$$

Each matrix element includes the Boltzmann factor arising from the bonds between the layers and the in-plane bonds of the first layer. The count is governed by the number of ways that the flipped spins in the second layer can be added to those in the first layer. Two terms arise in the bottom right-hand element because the pairs of spins in the neighbouring layers can have either one or two axial connections. Similarly, the matrix which adds a layer of down (up) spins to a previous layer of up (down) spins is

$$\mathbf{M}_2 = \begin{pmatrix} \omega^{q_\perp} & q_\perp x^{-1}\omega^{q_\perp} \\ 2x^{-1}\omega^{2q_\perp - 2} & \{1 + 2(q_\perp - 1)x^{-2}\}\omega^{2q_\perp - 2} \end{pmatrix}.$$

The additional Boltzmann factor and count associated with the flipping of the first spin in the chain can be added by row vectors

$$\tilde{\mathbf{S}} = \begin{pmatrix} h_s & \dfrac{q_\perp}{2} h_s^2 \end{pmatrix}$$

if the chain begins at the the surface and

$$\mathbf{S} = \begin{pmatrix} x & \dfrac{q_\perp}{2} x^2 \end{pmatrix}$$

if it does not. (We shall need only the cases given when the spin is parallel to the surface field or its left-hand neighbour.) The matrix product is closed by column vectors which add the Boltzmann factors associated with the in-layer contribution and the bond to the right of the final flipped spin. These are

$$\mathbf{E}_1 = \begin{pmatrix} x\omega^{q_\perp} \\ x^2\omega^{2q_\perp - 2} \end{pmatrix} \qquad \mathbf{E}_2 = \begin{pmatrix} x^{-1}\omega^{q_\perp} \\ x^{-2}\omega^{2q_\perp - 2} \end{pmatrix}$$

if the final flipped spin is parallel or anti-parallel respectively to its nearest neighbour outside the chain.

It is not difficult to check that

$$\begin{aligned} f_{n+1} - f_n = {} & (\tilde{\mathbf{S}} - \mathbf{S})\mathbf{M}_1^{n-1}(\mathbf{E}_1 - \mathbf{E}_2) + \tilde{\mathbf{S}}\mathbf{M}_1^{n-1}(\mathbf{M}_1\mathbf{E}_2 - \mathbf{M}_2\mathbf{E}_1) + \mathbf{S}\mathbf{M}_1^{n-1}(\mathbf{M}_2 - \mathbf{M}_1)\mathbf{E}_1 \\ & + \sum_{p=0}^{\infty} \{\tilde{\mathbf{S}}\mathbf{M}_1^{n-1}(\mathbf{M}_1\mathbf{M}_2 - \mathbf{M}_2\mathbf{M}_1)\mathbf{M}_1^{p}\mathbf{E}_1 \\ & + \mathbf{S}\mathbf{M}_1^{n-1}(\mathbf{M}_2 - \mathbf{M}_1)\mathbf{M}_1^{p+1}\mathbf{E}_1\} \qquad n \geqslant 1 \end{aligned} \tag{23}$$

where the terms are ordered according to the axial length of the diagrams. Using (4) for h_s, the free-energy difference (23) can be expanded in terms of ω. Putting successive coefficients of powers of ω equal to zero gives an expression for the phase boundaries between successive interface phases. The coefficients α are listed in table 11.

The results in table 11 indicate that the pattern of the splitting of the phase boundaries is identical to that of the full Abraham model. For the simplified model we have been able to obtain results to $O(\omega^{11q_\perp - 10})$ showing that phases up to at least $n = 5$ are stable. Moreover, a comparison of the results of table 11 with the leading order terms of the expressions for $\alpha_1, \alpha_2, \ldots$ derived for the full model in section 4 shows that they agree to leading order. Therefore it seems that the important physics is not lost in the simplification. Hence our

Table 11. The coefficients which appear in the expansion of the phase boundaries $(h_s)_{n+1:n}$ of the simplified model.

Boundary					Order
2 : 1	3 : 2	4 : 3	5 : 4	6 : 5	
1	1	1	1	1	$\omega^{q_\perp}$
$q_\perp x^2$	$q_\perp x^2$	$q_\perp x^2$	$q_\perp x^2$	$q_\perp x^2$	$\omega^{2q_\perp-2}$
1	1	1	1	1	$\omega^{2q_\perp}$
$\frac{1}{2}q_\perp(1+O(x^2))$	$q_\perp x^2(1-2x^2)$	$q_\perp x^2(1-2x^2)$	$q_\perp x^2(1-2x^2)$	$q_\perp x^2(1-2x^2)$	$\omega^{3q_\perp-4}$
	$2q_\perp x^2$	$2q_\perp x^2$	$2q_\perp x^2$	$2q_\perp x^2$	$\omega^{3q_\perp-2}$
	1	1	1	1	$\omega^{3q_\perp}$
		$q_\perp x^2(1-2x^2)$	$q_\perp x^2(1-2x^2)$	$q_\perp x^2(1-2x^2)$	
	$\frac{1}{2}q_\perp(1+O(x^2))$	$(1-2x^2(q_\perp+1))$	$(1-2x^2(q_\perp+1))$	$(1-2x^2(q_\perp+1))$	$\omega^{4q_\perp-6}$
		$2q_\perp x^2(1+$			
		$x^2(q_\perp-2))$	$2q_\perp x^2(1+x^2(q_\perp-2))$	$2q_\perp x^2(1+x^2(q_\perp-2))$	$\omega^{4q_\perp-4}$
		$3q_\perp x^2$	$3q_\perp x^2$	$3q_\perp x^2$	$\omega^{4q_\perp-2}$
		1	1	1	$\omega^{4q_\perp}$
			$q_\perp x^2(1-2x^2)((1-2x^2)^2-$	$q_\perp x^2(1-2x^2)((1-2x^2)^2-$	
		$\frac{1}{2}q_\perp(1+O(x^2))$	$6q_\perp x^2(1-2x^2)+4{q_\perp}^2x^4)$	$6q_\perp x^2(1-2x^2)+4{q_\perp}^2x^4)$	$\omega^{5q_\perp-8}$
			$2q_\perp x^2((1-2x^2)^2-{q_\perp}^2x^4)$	$2q_\perp x^2((1-2x^2)^2-{q_\perp}^2x^4)$	$\omega^{5q_\perp-6}$
			$3q_\perp x^2(1-2x^2+2q_\perp x^2)$	$3q_\perp x^2(1-2x^2+2q_\perp x^2)$	$\omega^{5q_\perp-4}$
			$4q_\perp x^2$	$4q_\perp x^2$	$\omega^{5q_\perp-2}$
			1	1	$\omega^{5q_\perp}$
				$q_\perp x^2(1-2x^2)(1-2x^2$	
			$\frac{1}{2}q_\perp(1+O(x^2))$	$-2q_\perp x^2)((1-2x^2)^2-$	$\omega^{6q_\perp-10}$
				$10q_\perp x^2(1-2x^2)+4{q_\perp}^2x^4)$	

results provide evidence that the pattern in the exact model persists with increasing n and that at least a large number of phases are stable. Because the simplified model retains the diagrams driving the splitting of the phase boundaries, we may conclude that these are connected diagrams with at most two spins per layer.

7. Mean-field theory

In this section we take the mean-field limit of the low-temperature series expansion. The aim is to see whether the layering transitions persist and hence to ascertain whether mean-field theory gives a qualitatively correct representation of the phase diagram at low temperatures.

We restrict ourselves to taking the mean-field limit within the planes, that is $q_\perp \to \infty$ with $q_\perp J_0$ fixed. In this limit the quantity $\tilde{\omega} \equiv \omega^{q_\perp}$ is constant. Using

$$\omega^{-2} - 1 = \frac{-2\ln\tilde{\omega}}{q_\perp} + \frac{2(\ln\tilde{\omega})^2}{{q_\perp}^2} + O\left(\frac{1}{{q_\perp}^3}\right) \tag{24}$$

and taking the limit $q_\perp \to \infty$, equation (4) may be rewritten

$$h_s = x\left(1 + \alpha_1\tilde{\omega} - \frac{2\alpha_2}{q_\perp}\tilde{\omega}^2\ln\tilde{\omega} + (\alpha_2+\alpha_3)\tilde{\omega}^2 + \frac{8\alpha_4+2\alpha_5}{{q_\perp}^2}\tilde{\omega}^3(\ln\tilde{\omega})^2 - \frac{4\alpha_4+2\alpha_5}{q_\perp}\tilde{\omega}^3\ln\tilde{\omega} + (\alpha_4+\alpha_5+\alpha_6)\tilde{\omega}^3 + \cdots\right). \tag{25}$$

This boundary will only behave sensibly in the mean-field limit if α_1, $\alpha_2+\alpha_3$, $\alpha_4+\alpha_5+\alpha_6 \sim O(1)$; $\alpha_2, 4\alpha_4+2\alpha_5 \sim O(q_\perp)$ and $8\alpha_4+2\alpha_5 \sim O({q_\perp}^2)$. It can be seen from (11)–(17) that this is indeed the case providing a useful check on the calculations.

Using the expressions (11)–(17) for the αs the coefficients in (25) can easily be calculated. The $n = 1$ phase becomes stable $O(\tilde{\omega}^2 \ln \tilde{\omega})$ and the $n = 2$ phase $O(\tilde{\omega}^3 \ln \tilde{\omega})$. Therefore, at least to this order of the expansion, the qualitative behaviour of the model remains unchanged in the mean-field limit.

8. Discussion

In this paper we have used a low-temperature series expansion to study the phase diagram of the Abraham model in dimensions $d \geqslant 3$. We have been able to show that there are at least four layering transitions and presented arguments based on a simplified version of the model that there are a large, possibly infinite number of transitions beyond these.

The calculation proved much more difficult than a similar approach to complete wetting in an Ising model [4]. In that case the *leading* term in the free-energy difference $f_{n+1} - f_n$ was responsible for stabilizing the phase $n+1$ for all n. In terms of diagrams the calculation of the contribution from single axial chains of length n sufficed to prove that an infinite number of layering transitions were stable. For the Abraham model, however, the number of terms in the free-energy differences needed to establish the stability of a phase n increases with n. Hence the calculation rapidly becomes prohibitively difficult and we were not able to formulate a general argument showing how successive states are stabilized.

Armitstead and Yeomans [6] considered a solid-on-solid version of the Abraham model where overhangs of the interface and bulk fluctuations are prohibited. This model is equivalent to a highly anisotropic limit of the system considered here. They again found that diagrams more complicated than single axial chains were needed to break the degeneracy of neighbouring phases. However, because the solid-on-solid condition provides a strong restriction on the number of allowed diagrams they were nevertheless able to prove the existence of an infinite number of layering transitions.

Acknowledgments

CLO'D acknowledges a studentship from the Department of Education of Northern Ireland. JMY acknowledges an SERC Advanced Fellowship.

References

[1] Abraham D B 1980 *Phys. Rev. Lett.* 44 1165
[2] de Oliveira M J and Griffiths R B 1978 *Surf. Sci.* 71 687
[3] Pandit R, Schick M and Wortis M 1982 *Phys. Rev.* B 26 5112
[4] Duxbury P M and Yeomans J M 1985 *J. Phys. A: Math. Gen.* 18 L983
[5] Fisher M E and Selke W 1982 *Phil. Trans. R. Soc.* 302 1
[6] Armitstead K and Yeomans J M 1988 *J. Phys. A: Math. Gen.* 21 159
[7] Binder K and Landau D P 1988 *Phys. Rev.* B 37 1745
[8] Domb C 1960 *Adv. Phys.* 9 149
[9] O'Donnell C L 1993 *PhD Thesis* University of Oxford
[10] Yeomans J M and Fisher M E 1984 *Physica* 127A 1